



**University of
Zurich^{UZH}**

**Zurich Open Repository and
Archive**

University of Zurich
University Library
Strickhofstrasse 39
CH-8057 Zurich
www.zora.uzh.ch

Year: 2014

Weathering of granite from the Damma glacier area: the contribution of cyanogenic bacteria

Wongfun, Nuttakan ; Plötze, Michael ; Furrer, Gerhard ; Brandl, Helmut

Abstract: The dissolution potential of five cyanogenic bacteria was studied at 25 °C during 32 days using granite material from the Damma glacier (Central Alps, Switzerland) as the sole source of nutrients. The bacterial species *Pseudomonas fluorescens* and *Pseudomonas* sp. CCOS 191 were the most effective to exudate various organic acids and consequently mobilised Fe. The molecular mechanisms include both, proton- promoted and ligand-promoted dissolution, preferentially at pH below 5 and in the pH range between 5.0 and 5.8, respectively. In addition, bacterially produced cyanide plays a minor role through the formation of soluble hexacyanoferrate complexes. To our knowledge, this study is the first that reveals the direct measurement of metal-cyanide complexes formed during biotic granite weathering.

DOI: <https://doi.org/10.1080/01490451.2013.802396>

Posted at the Zurich Open Repository and Archive, University of Zurich

ZORA URL: <https://doi.org/10.5167/uzh-80254>

Journal Article

Accepted Version

Originally published at:

Wongfun, Nuttakan; Plötze, Michael; Furrer, Gerhard; Brandl, Helmut (2014). Weathering of granite from the Damma glacier area: the contribution of cyanogenic bacteria. *Geomicrobiology Journal*, 31(2):93-100.

DOI: <https://doi.org/10.1080/01490451.2013.802396>

Weathering of granite from the Damma glacier area: the contribution of cyanogenic bacteria

Nuttakan Wongfun¹, Michael Plötze², Gerhard Furrer¹ and Helmut Brandl³

¹ Institute of Biogeochemistry and Pollutant Dynamics, Department of Environmental Systems Science, ETH Zurich, Zurich, Switzerland

² Institute for Geotechnical Engineering, Department of Civil, Environmental and Geomatic Engineering, ETH Zurich, Zurich, Switzerland

³ Institute of Evolutionary Biology and Environmental Studies, University of Zurich, Zurich, Switzerland

ABSTRACT

The dissolution potential of five cyanogenic bacteria was studied at 25 °C during 32 days using granite material from the Damma glacier (Central Alps, Switzerland) as the sole source of nutrients. The bacterial species *Pseudomonas fluorescens* and *Pseudomonas* sp. CCOS 191 were the most effective to exudate various organic acids and consequently mobilised Fe. The molecular mechanisms include both, proton-promoted and ligand-promoted dissolution, preferentially at pH below 5 and in the pH range between 5.0 and 5.8, respectively. In addition, bacterially produced cyanide plays a minor role through the formation of soluble hexacyanoferrate complexes. To our

knowledge, this study is the first that reveals the direct measurement of metal-cyanide complexes formed during biotic granite weathering.

Keywords cyanogenic bacteria, granite, dissolution, cyanide, organic acids

INTRODUCTION

Climate changes potentially exacerbate glaciers to retreat along with a loss of permafrost. The European Alpine glaciers showed 35% areal loss within two decades, in particular up to more than 80 m of thickness has been lost from the Swiss Alps (Meier et al. 2003; Paul and Haeberli 2008). Retreat of glaciers mainly uncovers steep slopes. Glacier sediment and moraine debris are reworked and transported along the valleys (Anderson 2007). Newly exposed rock surfaces can be considered as pioneer ecosystems and provide nutrient sources to plants and microbial life (Southam 2012). In return, plant and microbial succession as well as soil formation help to stabilise the surface moraine and prevent erosion.

The roles of microorganisms in mineral weathering have received wide recognition among geo-microbiologists (Bennett et al. 2001; Gorbushina 2007; Uroz et al. 2009; Brantley et al. 2011; Gadd et al. 2012). Soil microbes play an essential role in the environment by contributing to bioavailability of nutrients from primary minerals that are required not only for their own nutrition but also for that of plants. Even in harsh conditions of glacier forefields, microbes can endure due to their mineral-weathering

abilities (Hall et al. 2005; Frey et al. 2010; Brunner et al. 2011). Microbial weathering mechanisms include acidification, the effect of metabolites (e.g. organic acids, siderophores) and extracellular polymeric substances (EPS), and stimulation of redox reactions of metals in minerals. Recent work has revealed various aspects of microbe-granite interactions including release of nutrients from rock-forming minerals by microbial exudates (Liermann et al. 2000; Kalinowski et al. 2000; Uroz et al. 2007; Wu et al. 2008; Balland et al. 2010) and microbial colonisation patterns (Barker et al. 1998; Song et al. 2007). Available knowledge of bacterially mediated granite weathering is fragmented and is characterised by large discrepancies due to heterogeneity of granite mineralogy, bacterial species, and experimental conditions. Furthermore, rates and mechanisms of bacterially mediated dissolution of granite were mainly derived from the molecular concepts of ligand-promoted dissolution, with the emphasis of bi-, tri- and tetra-dentate ligands (Furrer and Stumm 1986; Neaman et al. 2006; Hausrath et al. 2009).

Cyanide (CN^-) forms strong complexes with several transition metals (Hummel 2004). The lixiviant CN^- is considered as one of the oldest ligands in earth's history (Oparin 1953; Beck and Link 1977). During bacterial growth, cyanogenesis occurs in the secondary metabolism and can be stimulated by presence of glycine, ammonia, and iron and phosphate (Knowles and Bunch 1986; Rudolf von Rohr et al. 2009). However, the role of cyanogenesis in bacteria is still unclear (Dzombak et al. 2006).

The impact of CN^- on granite weathering has not been examined systematically. Some cyanogenic bacteria from the genus *Pseudomonas* were found to dissolve Cu

and Ni from minerals and ore samples (Faramarzi and Brandl 2006). Four bacterial isolates from the Damma glacier forefield showed paralleled formation of oxalic acid and CN^- , consequently enhanced Fe mobilisation (Frey et al. 2010). Nevertheless, the molecular mechanism of cyanide-promoted mineral dissolution was not clarified.

Our study aimed at the mechanisms of granite weathering in presence of cyanogenic bacteria. We investigated the mobilisation of elements under nutrient-limited condition, which contain sterile granite as the only source of nutrients. Further, we examined the weathering potential of well-known cyanogenic model strains and strains isolated from the rock surfaces of glacier forefields.

MATERIALS AND METHODS

Granite material

Granite from the Winterstock Mountain near the Damma glacier (Central Alps, Switzerland) was sampled in winter 2007. The glacial area is located in the Aar massif, where the bedrock is mainly composed of coarse-grained metagranite (Schaltegger 1990). The rock material was cut off with a hammer from the bedrock. The material was crushed to a grain size of <0.6 mm with a jawbreaker (Retsch BB51) and wet sieved to obtain the <63 μm fraction for further investigation. For the microbial dissolution experiment, the granite powder was sterilised by soaking in ethanol ($>99.5\%$) for one hour and subsequently drying at 150 $^{\circ}\text{C}$ overnight. Dry samples were kept in closed sterile containers in the desiccator. The specific surface area was 1.6 m^2/g measured by applying the N_2 -BET method (Quantachrome Autosorp 1 MP). Qualitative and

quantitative analysis of the mineral composition (Table 1) were carried out with X-ray powder diffraction (XRD, BRUKER AXS D8 Advance) and Rietveld refinement with the AutoQuan/BGMN code (Bergmann and Kleeberg 1998). The chemical compositions (Table 1) of major mineral phases were analysed with the electron probe microanalysis (EPMA, JEOL JXA-8200) equipped with a SE detector and a BSE detector in combination with an EDS analyser. The analysis was standardised using synthetic and natural oxides and silicates. The elemental composition of the granite (Table 2) was measured by X-ray fluorescence spectroscopy (XRF, Spectro X Lab 2000 Spectrometer).

Bacterial strains and preparation of inocula

Five cyanogenic bacterial strains, *Pseudomonas* sp. CCOS 191 (Culture Collection of Switzerland, strain CCOS 191), *Pseudomonas fluorescens* CHA0 (donation of Monika Maurhofer, Plant Pathology Group, ETH Zurich), the green fluorescent protein-containing strain *Pseudomonas putida* KT2442 (RP4:gfp) (donation of Gabriella Pessi, Institute of Plant Biology, University of Zurich), and the strains *Janthinobacterium* sp. and *Leifsonia* sp. isolated from the Damma glacier forefield (Frey et al. 2010; Lapanje et al. 2012), were cultivated for three days in sterile LB medium (Bertani 1951). Cells were harvested by washing and re-suspended three times as following: after centrifugation at 5000 rpm for 5 minutes, the supernatants were discarded and the remaining solids were re-suspended and vigorously mixed in a sterile NaCl solution (0.9% w/v).

Biotic granite dissolution

Acid-washed 250 ml Erlenmeyer flasks filled with 100 ml of minimal growth medium (3.3 mmol L⁻¹ D-glucose monohydrate, 1.9 mmol L⁻¹ NH₄Cl in nanopure water, initial pH adjusted to 6.5 with 1 mol L⁻¹ NaOH) was supplemented with 1 g sterile granite, inoculated with 2 ml of washed cultures, and incubated at 25 °C (90 rpm). Abiotic granite dissolution was also performed as a control. From each microcosm, aliquots were sampled at regular time intervals (0, 1, 2, 8, 16, 24, 32 d). The sampled aliquots were immediately filtered through 0.2 µm nylon filters. For further analysis, three fractions were preserved differently. The first fraction was kept at -20 °C for metabolite analysis. The second fraction was basified using NaOH (1% v/v, 1 mol L⁻¹) for the free CN⁻ analysis. In the last fraction, the pH was measured with a microelectrode (Metrohm), and the solution was acidified by HNO₃ (3% v/v, 65%) for elemental analysis.

Chemical analyses

Metabolites (organic acids and hexacyanoferrate complexes) were analysed using high-pressure liquid chromatography (HPLC, Bischoff) coupled with a UV/VIS detector (Metrohm Bischoff Lambda 1010). Organic acids were separated at 40 °C on an Aminex HPX-87H column (Biorad) using 5 mmol L⁻¹ H₂SO₄ as an eluent (0.6 ml min⁻¹). Peaks for acetate, citrate, gluconate, lactate, oxalate, and pyruvate were detected at 210 nm (Rudolf von Rohr et al. 2009). Hexacyanoferrate complexes (Fe^{II}[CN]₆⁴⁻ and Fe^{III}[CN]₆³⁻) were separated at 40 °C on a hydrophobic C-18 column (Faramarzi et al. 2004). The

eluent consisted of 25% w/v acetonitrile, 150 mmol L⁻¹ ortho-phosphoric acid, 2.34 mmol L⁻¹ sodium perchlorate monohydrate and 90 mmol L⁻¹ tetrabutylammonium hydroxide (TBAOH) and was adjusted to pH 7.3 by NaOH. The flow rate was 1 ml min⁻¹. Peaks for Fe^{II}[CN]₆⁴⁻ and Fe^{III}[CN]₆³⁻ were detected at 225 nm. Quantitative free CN⁻ determination was based on the methemoglobin method (Baumeister and Schievelbein 1971) in a 96-well microtiter plate (NuncloTM) using a plate reader at 427 nm (Bücher Biotec AG Spectramax M2) (Rudolf von Rohr et al. 2009). Qualitative free CN⁻ measurement was performed using the tetrabase filter paper method (Castric and Castric 1983). Bacterial isolates were cultivated especially for qualitative CN⁻ test in sterile LB medium with the addition of 1 mmol L⁻¹ glycine. Indicator papers were prepared by dissolving 50 mg copper (II) acetoacetate and 50 mg tetramethyl diaminodiphenylmethane in 15 ml chloroform. The filter paper was soaked with the solution and air-dried. Strips were positioned in the headspace of the batch cultures. Elemental releases from granite were analysed from acidified aliquots using inductively coupled plasma optical emission spectrometry (ICP-OES, Varian Vista-MPX spectrometer). The results achieved from ICP-OES analysis were corrected for the remaining volume in the microcosms and the loss of elemental mass during sampling using the following equation (Wu et al. 2007):

$$C_{j,i}^* = \frac{C_{j,i}[V_0 - jV_s] + \sum_{h=1}^j C_{h,i}V_s}{V_0} \quad (1)$$

where $C_{j,i}^*$ is the corrected concentration (mol L⁻¹) of element i in the j^{th} sample, $C_{j,i}$ is the measured concentration, V_0 is the initial fluid volume (0.1 L), V_s is the sampling volume

(0.007 L), and the term $\sum_{h=1}^j C_{h,i} V_s$ accounts for the mass of element i extracted during sampling.

RESULTS

Changes in pH values

The cultures contained unbuffered minimal growth medium with initial pH 6.5. A drastically decrease was observed in every culture within 8 days of granite dissolution. After 8 days towards the end of the experiment, pH ranges between 4.3 and 5.8 (Figure 1). *P. fluorescens* lowered the pH effectively already at the first day of the experiment. Although *Leifsonia* sp., and the abiotic control showed a small increased pH at the first two days, a decreasing trend occurred toward the end of the experiments.

Production of metabolites

Figure 2 shows the formation of organic acids after 8 days of granite dissolution. The occurrence and concentrations varied among the various bacterial strains. No metabolites were observed in abiotic controls. We detected significantly high concentrations of citrate ($772 \mu\text{mol L}^{-1}$) and pyruvate ($545 \mu\text{mol L}^{-1}$) in the culture of *P. fluorescens*. Conversely, pyruvate was observed in all cultures in a concentration range between 10 and $545 \mu\text{mol L}^{-1}$. *Pseudomonas* sp. CCOS 191 exuded all investigated acids in which gluconate and citrate attributed to 64% and 22% of the total concentration, respectively. By exudation of all measured acids similar to *Pseudomonas* sp. CCOS 191, *Janthinobacterium* sp. formed small amounts of acids ranging from 0.6

to $40 \mu\text{mol L}^{-1}$. Instead, *P. putida* exuded only pyruvate ($319 \mu\text{mol L}^{-1}$) at day 8, although we observed small quantities of citrate, lactate and oxalate in the early state of bacterial growth (data not shown).

Free CN^- and hexacyanoferrate complexes ($\text{Fe}^{\text{II}}[\text{CN}]_6^{4-}$ and $\text{Fe}^{\text{III}}[\text{CN}]_6^{3-}$) were analysed by HPLC. The species $\text{Fe}^{\text{III}}[\text{CN}]_6^{3-}$ was not present in any culture. The culture of *P. fluorescens* showed the presence of both free CN^- and $\text{Fe}^{\text{II}}[\text{CN}]_6^{4-}$ (Table 3). Whereas, only the $\text{Fe}^{\text{II}}[\text{CN}]_6^{4-}$ complex was observed in the culture of *Pseudomonas* sp. CCOS 191. Neither free CN^- nor $\text{Fe}^{\text{II}}[\text{CN}]_6^{4-}$ complexes were found in the other cultures. Similar to the quantitative tests, bacterial capability of cyanogenesis was observed through the qualitative analysis in glycine-LB medium. Only *Pseudomonas* sp. CCOS 191 and *P. fluorescens* showed significant positive results.

Release of elements

Elemental mobilisations in the bacterial cultures were clearly higher than those in the abiotic control at the end of the experiment, except in the case of P, where only *P. fluorescens* and *Pseudomonas* sp. CCOS 191 showed distinct effects (Figure 3). The most pronounced influence of bacteria was shown in case of Fe mobilisation (Figure 3D), in particular the cultures of *P. fluorescens* and *Pseudomonas* sp. CCOS 191. Within one day, released Fe concentration in the culture of *P. fluorescens* was almost two orders of magnitude higher than those in the other cultures and the abiotic control. Although *Leifsonia* sp. showed the lowest potential of Fe mobilisation, released Fe concentration was still twofold higher than those of the abiotic control after 32 days. The

cultures of *P. fluorescens* and *Pseudomonas* sp. CCOS 191 also showed prominent effects regarding other elements. The strain *P. fluorescens* showed highest efficiency to mobilise Ca and Mg, whereas *Pseudomonas* sp. CCOS 191 was able to mobilise Al and P efficiently. On the other hand, *P. putida*, *Janthinobacterium* sp., and *Leifsonia* sp. mobilised relatively small quantities of Al and Mg. The concentrations of K clustered among those released from biotic dissolution. After 2 days, bacteria mobilised K from the granite at least twofold higher than those of the abiotic control.

Table 4 shows the results of the mobilisation potential in terms of elemental budget and rates of Fe mobilisation, based on corrected concentrations. Elemental release rates were calculated using the linear rate equation (Wu et al. 2008):

$$R_i^l = \frac{dC_i^*}{dt} \frac{V_0}{Am} \quad (2)$$

where R_i^l is the linear release of element i ($\text{mol m}^{-2} \text{s}^{-1}$), dC_i^*/dt is the slope of the line describing C_i^* versus time, V_0 is the initial fluid volume, A is the specific surface area, and m is the mass of granite powder. We assume similar loss of fluid due to evaporation in all microcosms including abiotic experiments from the same batches.

Rates of Fe mobilisation ranged from approximately 3×10^{-14} to $7 \times 10^{-11} \text{ mol m}^{-2} \text{s}^{-1}$. The fastest rate was calculated from the culture of *P. fluorescens* with up to 3% of the total Fe in the granite. Overall, high dissolving potential was shown in the cultures of *P. fluorescens* and *Pseudomonas* sp. CCOS 191.

DISCUSSION

Aside from a supply of glucose as C source and NH_4Cl as N source, granite powder was the only source of nutrients to support bacterial growth. Our results reveal that bacteria were able to grow in nutrient-limited conditions and to mobilise nutrients from granite.

A change in pH is usually observed in bacterial cultures and can be used as an indirect indicator of bacterial growth. In the early stage of the experiment, pH changes may be influenced by a fast dissolution of fine granite particles created by sample preparation (crushing and grinding processes). A significant pH decrease in biotic microcosms (Figure 1) can be explained by protons from bacterially produced organic acids (Figure 2) as discussed by Wu et al. (2008). An alternative source of protons attributes to the NH_4^+ -bearing medium. A stoichiometric coupling of bacterial uptake of NH_4^+ and extrusion of H^+ cause a further acidification of the culture (Roos and Luckner 1984). The formation of CO_2 during bacterial metabolism can lower the solution pH. Several authors noted increasing dissolution rates in correlation with decreasing pH (Liermann et al. 2000; Balland et al. 2010; Frey et al. 2010).

We selected released Fe as an indicator of granite dissolution due to its reliable fit (R^2 value greater than 0.9) and its strong affinity to organic ligands and CN^- . Several bacterial strains were reported to show a high potential to enhance Fe dissolution (Loper and Henkels 1997; Kalinowski et al. 2000). Bacterial isolates from the Damma glacier forefield revealed to mobilise between 15 and $140 \mu\text{mol L}^{-1}$ of Fe (Frey et al. 2010; Lapanje et al. 2012).

Bacterial organic acids can enhance the dissolution of silicate minerals by increasing mineral solubility (Bennett et al. 2001; Barker et al. 1997). The contribution of organic acids to mineral weathering is based on two molecular mechanisms: proton-promoted and ligand-promoted dissolution (Furrer and Stumm 1986). Proton-promoted dissolution results from the protonation of mineral surface sites and might be particularly enhanced in the case of nearby bacterial cells, with their acidic exudates. In addition, ligand-promoted dissolution results most efficient from the formation of surface-chelate complexes that form five- and six-membered rings. The latter contribution is most important under moderately acidic conditions, where proton-promoted dissolution is less pronounced.

In presence of chelating agents (e.g. citrate), the formation of chelate complexes is competitive between Fe cations and protons. The stability of Fe chelate complexes is pH dependent. Our results show that dissolution processes occurred simultaneously at pH between 4.3 and 6.7 depending on pH and ligand concentration. At near-neutral pH, where mineral surface are little or not protonated, ligands polarise and loosen the bonds between the complexed metal centres and the mineral lattice. Under acidic conditions, the proton-promoted dissolution may become super-imposed on the effects by ligands (Furrer and Stumm 1986). We observed negative correlations between pH and released Fe in all cultures (Figure 4). In most cases, elevated Fe concentrations suggest proton-promoted dissolution at pH <5, except in the culture of *Pseudomonas* sp. CCOS 191. In this case, the super-imposed effect was observed between pH 5.0 and 5.8. Similar

cases were reported in biotic dissolution of apatite (Welch et al. 2002) and biotite-phlogopite (Balland et al. 2010).

The two main sources of Fe in the Damma granite are epidote and biotite (Table 1). Although, proton-promoted dissolution of biotite can be strongly influenced by K concentration in solution (Kiczka et al. 2010), elevated K concentrations during 32 days of the experiments did not influence the mobilisation of Fe. The concentrations of released K (Figure 3C) were found similar in all cultures, while released Fe (Figure 3D) was significantly high in the cultures of *Pseudomonas* sp. CCOS 191 and *P. fluorescens*.

The effect of ligand-promoted dissolution depends on the strength of complexation and concentration of exuded ligands. Assuming 1:1 complexation stoichiometry, the ratios between the total concentration of acids and released cations (Table 5) were significant at day 8. The observed ratios (>1) of ligands to cations in solution suggest that the organic ligands are the key factor for the cation mobilisation. In case of a ratio <1 , substantial amounts of cations are released into the solution without complexation by ligands. Organic acids only indirectly influence the dissolution processes through surface protonation. According to the high strength of the cation-ligand complexes, citrate is the most effective ligand for divalent and trivalent cations, in particular Fe (Neaman et al. 2006; Brunner et al. 2011). Though Table 5 shows high ratios of citrate:Fe (>1) in the cultures of *P. fluorescens* and *Leifsonia* sp., citrate effectively mobilised cations only in the culture of *P. fluorescens* (citrate:cations >1). In the latter culture, the ratios of citrate:Fe and citrate:total cations were 3.6 and 1.9,

respectively. This may be explained by the high amount of the citrate exuded by *P. fluorescens* (0.8 mmol L⁻¹, up to >60% of the total acid concentration). In contrast, the strain *Leifsonia* sp. inefficiently mobilised Fe, despite a considerably high ratio of citrate:Fe (1.6). This suggests that not only the affinity, but also the quantity of the ligand is important to prevent the precipitation of secondary phases (such as Fe oxyhydroxides) and maintain Fe in the solution (Neaman et al. 2006; Balland et al. 2010). The quantity of exuded organic ligands, which affects mineral dissolution, varies from ~0.5 mmol L⁻¹ (Vandevivere et al. 1994) to at least 1 mmol L⁻¹ (Drever and Stilling 1997).

Besides exudation of organic ligands that enhance granite dissolution, *P. fluorescens* and *Pseudomonas* sp. CCOS 191 also produced CN⁻. Although the role of CN⁻ in bacterial growth is unclear and cyanide may play only a minor role in the dissolution mechanisms, several studies reported cyanogenesis during bacterial secondary metabolism (Knowles and Bunch 1986; Dzombak et al. 2006). The extent of CN⁻ production in our experiment was two orders of magnitude lower than those of organic acids (Figure 2). Nevertheless we detected measurable concentration of Fe^{II}[CN]₆⁴⁻ complexes during the experiments. Despite the fact that the total released Fe from the granite was approximately 30 to 40 times greater than the concentration of Fe-cyanide complexes, the occurrence of these complexes suggests that cyanide may also contribute to the mobilisation of iron. Previous studies (Faramarzi et al. 2004; Faramarzi and Brandl 2006; Frey et al. 2010) only revealed a correlation of cyanide and the concentration of metals released from the minerals.

Arguably, cyanide as a monodentate ligand, the contribution to mineral dissolution is very slightly through a ligand-promoted dissolution mechanism (Furrer and Stumm 1986; Neaman et al. 2006). However, from a chemical point of view, CN^- is a strong complexing agent, in particular with Fe cations. The stability constants of $\text{Fe}[\text{CN}]_6$ ($\log K_{\text{Fe}}^{\text{III}}=43.9$ and $\log K_{\text{Fe}}^{\text{II}}=36.9$; Hummel 2004) indicate that the Fe-cyanide complexes are much stronger than those with organic ligands. This implies that CN^- may increase Fe mobilisation through complexation of released Fe. The adsorption of cyanide on several metal-oxide surfaces was described as a mixing of covalent and ionic bonds (Ample et al. 2004). In the culture of *P. fluorescens*, the Fe-cyanide complexes might be formed after proton-induced mobilisation since pH values of 4.4 were observed. The solubility of Fe-cyanide complexes is low at $\text{pH} < 6$ (Meeussen et al. 1992). When bacteria exuded more cyanide, more Fe-cyanide complexes were formed. Therefore the subsequent “Fe-trapping” by CN^- indirectly drives Fe mobilisation from granite as a consequence of increasing thermodynamic solubility. Our results suggest a contribution of cyanide to the weathering of granite, which however, is minor in comparison to the total contribution of organic ligands.

Pseudomonas putida, *Janthinobacterium* sp., and *Leifsonia* sp. have been reported as cyanogenic strains (Flaishman et al. 1996; Frey et al. 2010). However, CN^- was absent in our case. Siderophore formation was not addressed in this study. Although siderophores can form complexes with Fe and may influence Fe dissolution in addition to cyanide (Kalinowski et al. 2000; Kraemer 2004), no siderophores were

detected in a wide range of bacterial isolates from glacier forefields, including *Pseudomonas* sp., *Janthinobacterium* sp., and *Leifsonia* sp. (Frey et al. 2010).

CONCLUSIONS

In conclusion, cyanogenic bacteria can influence granite dissolution through various mechanisms. Among bacterial species, in our case *P. fluorescens* exhibits the highest potential of granite weathering and Fe mobilisation. Bacterial isolates from the glacier forefield exhibit a dissolution potential similar to that of *P. putida*. Besides the effect of protons and organic ligands that enhance elemental release from the mineral surfaces, CN^- adds a minor and indirect effect to the mobilisation of Fe from granite. We were able to identify the formation of Fe-cyanide complexes with direct measurements. However only a more comparative abiotic dissolution experiment in absence and presence of cyanide will allow quantifying the potential of cyanide on the weathering of granite.

ACKNOWLEDGEMENTS

We thank for assistance of Kurt Barmettler for the ICP-OES analysis, Dominique Gärtner for the granite preparation, Eric Reusser and Daniela Hunziker for the electron probe microanalysis. We benefited from the collaboration within the project cluster Biosphere-Geosphere interactions: Linking climate change, weathering, soil formation and ecosystem evolution (BiGLink) of the Competence Centre Environment and

Sustainability (CCES) of the ETH Domain. This study was financially supported by the Swiss National Science Foundation (Grant K-23K1-120601).

REFERENCES

- Ample F, Clotet A, Ricart JM. 2004. Structure and bonding mechanism of cyanide adsorbed on Pt(1 1 1). *Surf. Sci.* 558: 111-121.
- Anderson SP. 2007. Biogeochemistry of glacial landscape systems. In: *Annual Review of Earth and Planetary Sciences*. Palo Alto: Annual Reviews. P 375-399.
- Balland C, Poszwa A, Leyval C, Mustin C. 2010. Dissolution rates of phyllosilicates as a function of bacterial metabolic diversity. *Geochim Cosmochim Acta* 74: 5478-5493.
- Barker WW, Welch SA, Banfield JF. 1997. Biogeochemical weathering of silicate minerals. In: Banfield JF, Nealson KH, editors. *Review in Mineralogy*. Geomicrobiology: Interactions between microbes and minerals. Washington, DC: Mineralogical Society of America. P 391-428.
- Barker WW, Welch SA, Chu S, Banfield JF. 1998. Experimental observations of the effects of bacteria on aluminosilicate weathering. *Am Mineral* 83: 1551-1563.
- Baumeister R, Schievelbein H. 1971. Simple method for estimation of small amounts of cyanide in tobacco smoke and biological materials. *Fresen Z Anal Chem* 255: 362-363.
- Beck MT, Ling J. 1977. Transition-metal complexes in prebiotic soup. *Naturwissenschaften* 64: 91-91.

- Bennett PC, Rogers JR, Choi WJ, Hiebert FK. 2001. Silicates, silicate weathering, and microbial ecology. *Geomicrobiol J* 18: 3-19.
- Bergmann J, Kleeberg R. 1998. Rietveld analysis of disordered layer silicates. *Mater Sci Forum* 278-281: 300-305.
- Bertani G. 1951. Studies on lysogenesis. I. The mode of phage liberation by lysogenic *Escherichia coli*. *J. Bacteriol* 62: 293-300.
- Brantley SL, Megonigal JP, Scatena FN, Balogh-Brunstad Z, Barnes RT, Bruns MA, Van Cappellen P, Dontsova K, Hartnett HE, Hartshorn AS, Heimsath A, Herndon E, Jin L, Keller CK, Leake JR, McDowell WH, Meinzer FC, Mozdzer TJ, Petsch S, Pett-Ridge J, Pregitzer KS, Raymond PA, Riebe CS, Shumaker K, Sutton-Grier A, Walter R, Yoo K. 2011. Twelve testable hypotheses on the geobiology of weathering. *Geobiology* 9: 140-165.
- Brunner I, Ploetze M, Rieder S, Zumsteg A, Furrer G, Frey B. 2011. Pioneering fungi from the Damma glacier forefield in the Swiss Alps can promote granite weathering. *Geobiology* 9: 266-279.
- Castric KF, Castric PA. 1983. Method for rapid detection of cyanogenic bacteria. *Appl Environ Microbiol* 45: 701-702.
- Deer WA, Howie RA, Zussman J. 1992. An introduction to the rock-forming minerals. 2nd ed. China: Prentice Hall. 696 p.
- Drever JI, Stillings LL. 1997. The role of organic acids in mineral weathering. *Colloid Surfaces A* 120: 167-181.

- Dzombak DA, Ghosh RS, Young TC. 2006. Cyanide in Water and Soil: Chemistry, Risk, and Management. Boca Raton (FL): Taylor and Francis/CRC Press. 602 p.
- Faramarzi MA, Stagars M, Pensini E, Krebs W, Brandl H. 2004. Metal solubilization from metal-containing solid materials by cyanogenic *Chromobacterium violaceum*. J Biotechnol 113: 321-326.
- Faramarzi MA, Brandl H. 2006. Formation of water-soluble metal cyanide complexes from solid minerals by *Pseudomonas plecoglossicida*. FEMS Microbiol Lett 259: 47-52.
- Flaishman MA, Eyal Z, Zilberstein A, Voisard C, Haas D. 1996. Suppression of Septoria tritici blotch and leaf rust of wheat by recombinant cyanide-producing strains of *Pseudomonas putida*. Mol Plant Microbe Interact 9: 642-645.
- Frey B, Rieder SR, Brunner I, Plotze M, Koetzsch S, Lapanje A, Brandl H, Furrer G. 2010. Weathering-associated bacteria from the Damma glacier forefield: Physiological capabilities and impact on granite dissolution. Appl Environ Microbiol 76: 4788-4796.
- Furrer G, Stumm W. 1986. The coordination chemistry of weathering: I. Dissolution kinetics of δ - Al_2O_3 and BeO. Geochim Cosmochim Acta 50: 1847-1860.
- Gadd GM, Rhee YJ, Stephenson K, Wei Z. 2012. Geomycology: metals, actinides and biominerals. Environ Microbiol Rep 4: 270-296.
- Gorbushina AA. 2007. Life on the rocks. Environ Microbiol 9: 1613-1631.

- Hall K, Arocena JM, Boelhouwers J, Liping Z. 2005. The influence of aspect on the biological weathering of granites: observations from the Kunlun Mountains, China. *Geomorphology* 67: 171-188.
- Hausrath EM, Neaman A, Brantley SL. 2009. Elemental release rates from dissolving basalt and granite with and without organic acids. *Am J Sci* 309: 633-660.
- Hummel W. 2004. The influence of cyanide complexation on the speciation and solubility of radionuclides in a geological repository. *Environ Geol* 45: 633-646.
- Kalinowski BE, Liermann LJ, Givens S, Brantley SL. 2000. Rates of bacteria-promoted solubilization of Fe from minerals: a review of problems and approaches. *Chem Geol* 169: 357-370.
- Kiczka M, Wiederhold JG, Frommer J, Kraemer SM, Bourdon B, Kretzchmar R. 2010. Iron isotope fractionation during proton- and ligand-promoted dissolution of primary phyllosilicates. *Geochim Cosmochim Acta* 74: 3112-3128.
- Knowles CJ, Bunch AW. 1986. Microbial cyanide metabolism. *Adv Microb Physiol* 27: 73-111.
- Kraemer SM. 2004. Iron oxide dissolution and solubility in the presence of siderophores. *Aquat Sci* 66: 3-18.
- Lapanje A, Wimmersberger C, Furrer G, Brunner I, Frey B. 2012. Pattern of elemental release during the granite dissolution can be changed by aerobic heterotrophic bacterial strains isolated from Damma glacier central Alps. deglaciated granite sand. *Microb Ecol* 63: 865-882.

- Liermann LJ, Kalinowski BE, Brantley SL, Ferry JG. 2000. Role of bacterial siderophores in dissolution of hornblende. *Geochim Cosmochim Acta* 64: 587-602.
- Loper JE, Henkels MD. 1997. Availability of iron to *Pseudomonas fluorescens* in rhizosphere and bulk soil evaluated with an ice nucleation reporter gene. *Appl Environ Microbiol* 63: 99-105.
- Meeussen JCL, Keizer MG, Vanriemsdijk WH, Dehaan FaM. 1992. Dissolution behavior of iron cyanide (Prussian blue) in contaminated soils. *Environ Sci Tech* 26: 1832-1838.
- Meier MF, Dyurgerov MB, McCabe GJ. 2003. The health of glaciers: recent changes in glacier regime. *Climatic Change* 59: 123-135.
- Neaman A, Chorover J, Brantley SL. 2006. Effects of organic ligands on granite dissolution in batch experiments at pH 6. *Am J Sci* 306: 451-473.
- Oparin AI. 1953. The origin of life. New York: Dover Publications. 203 p.
- Paul F, Haeberli W. 2008. Spatial variability of glacier elevation changes in the Swiss Alps obtained from two digital elevation models. *Geophys Res Lett* 35: L21502.
- Roos W, Luckner M. 1984. Relationships between proton extrusion and fluxes of ammonium ions and organic acids in *Penicillium cyclopium*. *J Gen Microbiol* 130: 1007-1014.
- Rudolf von Rohr M, Furrer G, Brandl H. 2009. Effect of iron and phosphate on bacterial cyanide formation determined by methemoglobin in two-dimensional gradient microcultivations. *J Microbiol Methods* 79: 71-75.

- Schaltegger U. 1990. The Central Aar granite – highly differentiated calc-alkaline magnetism in the Aar massif (Central Alps, Switzerland). *Eur. J. Mineral* 2: 245-259.
- Song W, Ogawa N, Oguchi CT, Hatta T, Matsukura Y. 2007. Effect of *Bacillus subtilis* on granite weathering: A laboratory experiment. *Catena* 70: 275-281.
- Southam G. 2012. Minerals as substrates for life: The prokaryotic view. *Elements* 8: 101-106.
- Uroz S, Calvaruso C, Turpaul MP, Pierrat JC, Mustin C, Frey-Klett P. 2007. Effect of the mycorrhizosphere on the genotypic and metabolic diversity of the bacterial communities involved in mineral weathering in a forest soil. *Appl Environ Microbiol* 73: 3019-3027.
- Uroz S, Calvaruso C, Turpault M-P, Frey-Klett P. 2009. Mineral weathering by bacteria: ecology, actors and mechanisms. *Trends Microbiol* 17: 378-387.
- Vandevivere P, Welch SA, Ullman WJ, Kirchman DL. 1994. Enhanced dissolution of silicate minerals by bacteria at near-neutral pH. *Microb Ecol* 27: 241-251.
- Welch SA, Taunton AE, Banfield JF. 2002. Effect of microorganisms and microbial metabolites on apatite dissolution. *Geomicrobiol J* 19: 343-367.
- Wu L, Jacobson AD, Chen H-C, Hausner M. 2007. Characterization of elemental release during microbe-basalt interactions at T=28 degrees C. *Geochim Cosmochim Acta* 71: 2224-2239.
- Wu L, Jacobson AD, Hausner M. 2008. Characterization of elemental release during microbe-granite interactions at T=28 degrees C. *Geochim Cosmochim Acta* 72: 1076-1095.

TABLE CAPTIONS

Table 1 Mineralogical microanalysis of granite and percentage of mineral contribution to the total Fe pool. Chemical formula of individual minerals were analysed using EPMA. The asterisks indicate the exemptions, which were not analysed but taken from Deer et al. (1992). Mineralogical composition was analysed using XRD and Rietveld refinement.

Table 2 Elemental composition (% wt/wt or $\mu\text{g/g}$) of granite analysed using XRF.

Table 3 Production of metabolites ($\mu\text{mol L}^{-1}$) after 8 days of granite dissolution. Total organic ligand is the mean concentration of oxalate, citrate, gluconate, pyruvate and lactate produced in the batch microcosms ($n=3$). bdl = below detection limit.

Table 4 Linear rates of Fe mobilisation ($10^{-12} \text{ mol m}^{-2} \text{ s}^{-1}$) and percentage of mobilised Fe after 8 days of granite dissolution.

Table 5 Ratio of released acids and cations from granite dissolution (assuming 1:1 complexation). n.a. = not applicable due to the absence of citrate.

FIGURE CAPTIONS

Figure 1 pH changes during granite dissolution experiments (open circle = *Pseudomonas* sp. CCOS 191, closed circle = *P. fluorescens*, diamond = *P. putida*, triangle = *Janthinobacterium* sp., closed square = *Leifsonia* sp. and opened square = abiotic control without bacterial inoculate). Error bars represent one standard deviation from triplicate supernatant analyses.

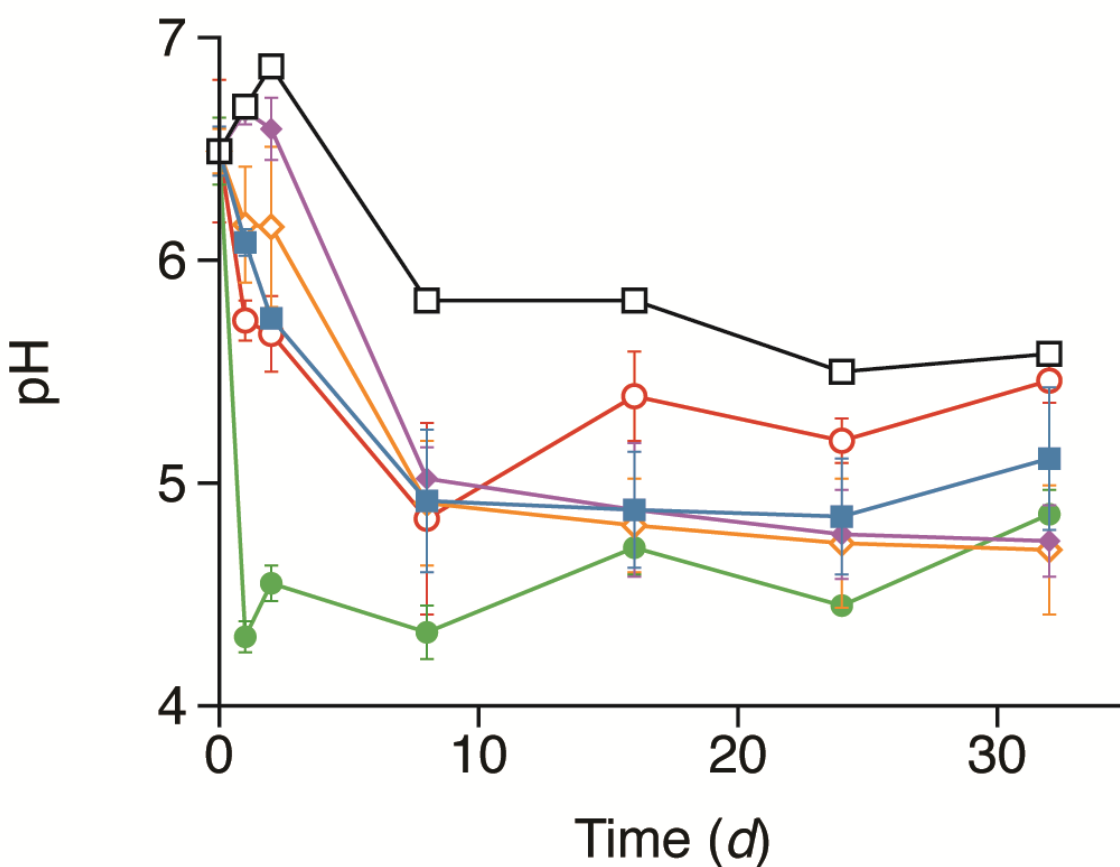


Figure 2 Concentration of metabolites ($\log \mu\text{mol L}^{-1}$) produced by bacteria after 8 days of granite dissolution. No metabolites were detected in abiotic granite dissolution.

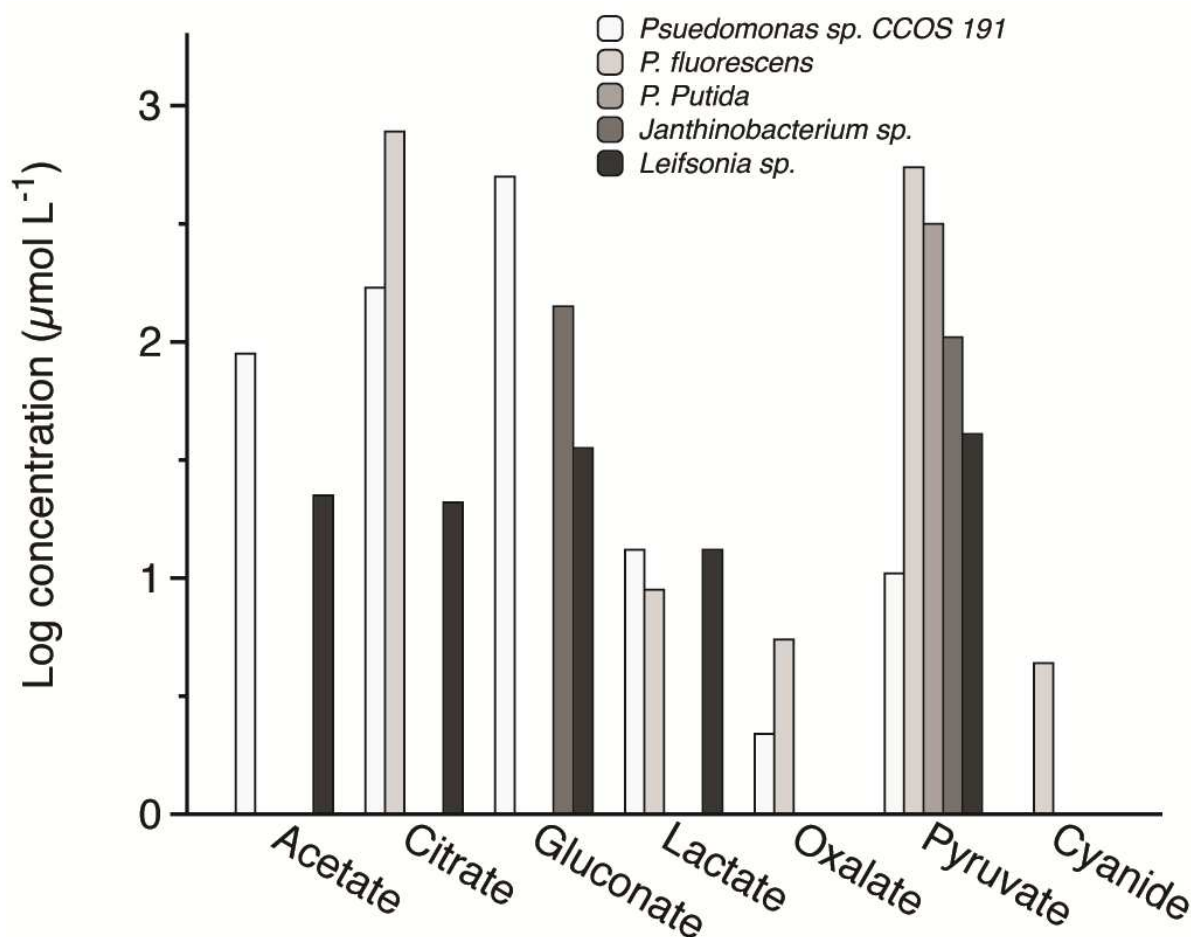


Figure 3 (A) Al, (B) Ca, (C) K, (D) Fe, (E) Mg, and (F) P releases ($\mu\text{mol L}^{-1}$) from granite dissolution experiments at 25 °C during 32 days in batch microcosm (open circle = *Pseudomonas sp. CCOS 191*, closed circle = *P. fluorescens*, diamond = *P. putida*, triangle = *Janthinobacterium sp.*, closed square = *Leifsonia sp.* and opened square =

abiotic control without bacterial inoculate). Error bars represent one standard deviation from triplicate supernatant analyses.

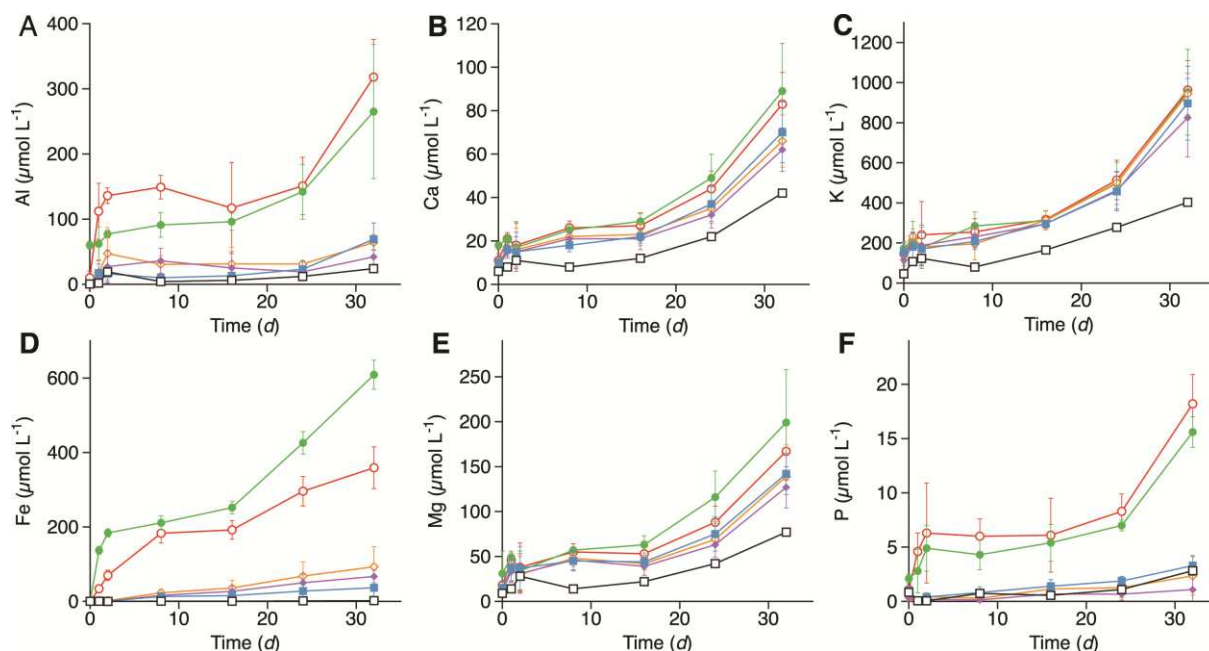


Figure 4 Released Fe ($\mu\text{mol L}^{-1}$) in granite dissolution as function of solution pH at 25 °C during 32 days in presence and in absence of bacteria (open circle = *Pseudomonas* sp. CCOS 191, closed circle = *P. fluorescens*, diamond = *P. putida*, triangle = *Janthinobacterium* sp., closed square = *Leifsonia* sp. and opened square = abiotic control without bacterial inoculate).

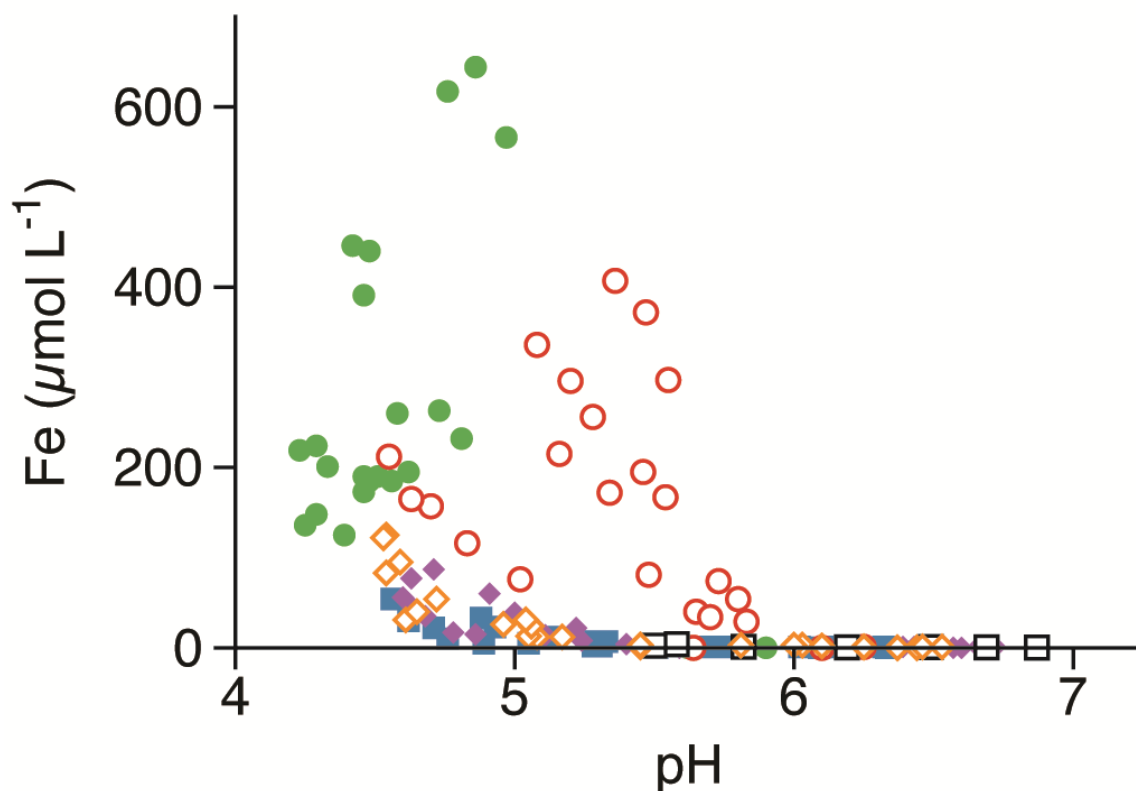


Table 1 Mineralogical microanalysis of granite and percentage of mineral contribution to the total Fe pool. Chemical formula of individual minerals were analysed using EPMA. The asterisks indicate the exemptions, which were not analysed but taken from Deer et al. (1992). Mineralogical composition was analysed using XRD and Rietveld refinement.

Mineral	Calculated chemical formula	wt/wt (%)	Fe contribution (%)
Plagioclase	$\text{Na}_{0.76}\text{Ca}_{0.18} [\text{Al}_{1.13}\text{Si}_{2.9}\text{O}_8] \text{Fe}_{0.03}$	28.0 ± 1.2	7.5
Quartz*	SiO_2	22.9 ± 0.7	-
Microcline	$\text{K}_{0.93}[\text{Al}_{1.02}\text{Si}_3\text{O}_8]\text{Na}_{0.01}$	16.6 ± 1.1	-
Muscovite	$\text{K}_{0.73}\text{Al}_{1.35} [\text{Si}_{3.19}\text{AlO}_{10}](\text{OH})_2\text{Mg}_{0.22}\text{Fe}_{0.22}$	11.5 ± 0.9	8
Biotite	$\text{K}_{0.95}\text{Mg}_{1.11}\text{Fe}^{\text{II}}_{1.38}\text{Ti}_{0.1}[\text{Si}_{2.88}\text{Al}_{1.5}\text{O}_{10}](\text{OH})_2$	8.6 ± 1.1	32
Epidote*	$\text{Ca}_2(\text{Al}, \text{Fe}^{\text{III}})\text{Al}_2\text{O OH} [\text{Si}_2\text{O}_7] [\text{SiO}_4]$	7.1 ± 0.7	38
Chlorite*	$(\text{Mg}, \text{Fe}^{\text{II}}, \text{Fe}^{\text{III}}, \text{Mn}, \text{Al})_{12} [(\text{Si}, \text{Al})_8\text{O}_{20}](\text{OH})_{16}$	3.2 ± 0.8	3.5

Apatite	$\text{Ca}_{9.97}(\text{PO}_4)_{5.37}\text{F}_{2.49}\text{Si}_{0.1}$	1.5 ± 0.5	-
Magnetite*	$\text{Fe}^{\text{II}}\text{Fe}^{\text{III}}_2\text{O}_4$	0.7 ± 0.3	11

Table 2 Elemental composition (% wt/wt or $\mu\text{g/g}$) of granite analysed using XRF.

Element (%) ($\mu\text{g/g}$)	Element ($\mu\text{g/g}$)	Element ($\mu\text{g/g}$)	Element
Si 22.7	P 972	V 48.6	Th 13.8
Al 6.4	Mn 780	Y 38.2	Hf 9.6
Fe 3.8	Zr 313	Nd 36.2	Ni 6.6
K 3.7	Sr 260	Cr 25.7	Cu 5.5
Ca 1.5	Rb 185	Nb 24.8	Sn 4.0
Na 1.4	S 101	Ga 22.1	As 3.8
Mg 1.0	Zn 71.4	Sm 20.2	Mo 2.7
Ti 0.3	Cl 69.6	Pb 18.9	Ge 1.5
Ba 0.2	Ce 54.9	La 17.7	Hg 1.0

Table 3 Production of metabolites ($\mu\text{mol L}^{-1}$) after 8 days of granite dissolution. Total organic ligand is the mean concentration of oxalate, citrate, gluconate, pyruvate and lactate produced in the batch microcosms ($n=3$). bdl = below detection limit.

Bacterial isolate	Total organic liand ($\mu\text{mol L}^{-1}$)	Free $\text{CN}^-_{(\text{aq})}$ ($\mu\text{mol L}^{-1}$)	$\text{Fe}^{\text{II}}[\text{CN}]_6$ ($\mu\text{mol L}^{-1}$)
<i>Pseudomonas</i> sp. CCOS 191	782	bdl	6.6
<i>P. fluorescens</i>	1331	4.4	5.8
<i>P. putida</i>	319	bdl	bdl
<i>Janthinobacterium</i> sp.	246	bdl	bdl
<i>Leifsonia</i> sp.	133	bdl	bdl

bdl

Bacterial isolate	Rate (10^{-12} mol m ⁻² s ⁻¹)	Fe mobilisation (%)
<i>Pseudomonas</i> sp. CCOS 191	19.35	2.69
<i>P. fluorescens</i>	70.97	3.10
<i>P. putida</i>	1.94	0.34
<i>Janthinobacterium</i> sp.	1.29	0.24
<i>Leifsonia</i> sp.	1.29	0.19
Abiotic control	0.03	0.06

Bacterial isolate	Total ligands: Total cations	Total ligands: Fe	Citrate : Total cations	Citrate: Fe
<i>Pseudomonas</i> sp. CCOS191	1.87	4.27	0.40	0.92
<i>P. fluorescens</i>	3.43	6.31	1.99	3.66
<i>P. putida</i>	2.53	13.87	n.a	n.a
<i>Janthinobacterium</i> sp.	2.03	15.38	n.a	n.a
<i>Leifsonia</i> sp.	1.51	10.14	0.24	1.60